Available online at www.sciencedirect.com

ScienceDirect

Ceramics International 40 (2014) 11485–11491

CERAMICS INTERNATIONAL

www.elsevier.com/locate/ceramint

# Piezoelectric properties of $Fe_2O_3$ doped $BiYbO_3$-$Pb(Zr,Ti)O_3$ high Curie temperature ceramics

Liang Shi[a,b], Boping Zhang[a,*], Qingwei Liao[b], Lifeng Zhu[a], Lei Zhao[a], Daibing Zhang[a], Dong Guo[b,**]

[a]School of Materials Science and Engineering, University of Science and Technology Beijing, Beijing 100083, China
[b]Institute of Acoustics, Chinese Academy of Sciences, Beijing 100190, China

Received 3 September 2013; received in revised form 8 October 2013; accepted 8 October 2013
Available online 17 October 2013

**Abstract**

The phase structure and electrical properties of $BiYbO_3$–$Pb(Zr,Ti)O_3$ + $x$(mol%)$Fe_2O_3$ (BY–PZT–$x$Fe) piezoelectric ceramics for applications at higher temperatures than those of PZT were investigated with a special emphasis on the influence of $Fe_2O_3$ content. All ceramics have a perovskite main phase with a tetragonal symmetry. The partial substitution of $Fe^{3+}$ with $Zr^{4+}$ and $Ti^{4+}$ in the B-site caused a shrinkage of the perovskite lattice and a decreased tetragonality ($c/a$) with increasing $x$ up to the solid solubility saturation at $x=0.4$. A lower tetragonality $c/a$, better grain morphology, and higher density as well as limited impurity phase were achieved at $x=0.4$ composition, all of which contribute to improved piezoelectric properties. The BY–PZT–$x$Fe ceramics showed a high Curie temperature $T_c$ up to 390 °C and good piezoelectric properties with $d_{33}$ reaching 175 pC/N at $x=0.4$.


*Keywords:* Piezoelectric ceramics; Curie temperature; Piezoelectricity

## 1. Introduction

Lead-containing piezoelectric ceramics based on $Pb(Zr,Ti)O_3$ (PZT) are widely used in various devices for application in communication, sensing, actuation, and energy harvesting, etc. In order to ensure the stability of piezoelectric properties, the safe usage temperature is generally limited to one half of their Curie temperatures $T_c$ [1,2]. Therefore, the piezoelectric devices used in the special high-temperature environment need high $T_c$. Generally, the $T_c$ of PZT ceramics is from 250 to 380 °C, so it is hard to meet the usage requirements of the special high-temperature piezoelectric devices. Commercial high-temperature piezoelectric sensor materials, such as $LiNbO_3$, usually has a complex production process and high cost [3].

A new high $T_c$ piezoelectric material system has been developed over the last few years in the $Bi(Me)O_3$–$PbTiO_3$ (Me = Sc, Yb, In) family [4–7]. Among them, $BiScO_3$–$PbTiO_3$ (BS–PT) ceramic has a high $T_c$ of 450 °C at a morphtropic phase boundary (MPB) composition, which is more than 100 °C higher than that of the current available PZT, along with a comparable piezoelectric constant $d_{33}$ of 460 pC/N with those of PZT [8]. Nevertheless, the practical application of the BS–PT ceramic is still seriously restricted because of the expensive $Sc_2O_3$. Untiring efforts have been made to search for alternatives with a high $T_c$, a practicable piezoelectric property, as well as low cost. Among the $BiMeO_3$–$PbTiO_3$ systems such as $BiYbO_3$–$PbTiO_3$ (BY–PT) [9], $BiInO_3$–$PbTiO_3$ [10], $BiGaO_3$–$PbTiO_3$ [11], and $BiFeO_3$–$PbTiO_3$ [12,13], the BY–PT system is an attractive one due to its high $T_c$ of > 620 °C [4]. However, it is usually difficult to obtain a pure perovskite structure for the BY–PT ceramics along with excessive pyrochlore impurity which seriously deteriorates piezoelectric properties $d_{33}$ to less than 28 pC/N regardless of the high $T_c$ over 530 °C [9]. Yang et al. [14] reported that the formation of pyrochlore phase could be suppressed effectively by adding $PbZrO_3$ in BY–PT ceramics, so as to improve greatly the piezoelectric constant $d_{33}$ from 18 pC/N for $0.1BiYbO_3$–$0.9PbTiO_3$ to 223 pC/N for the $0.055BiYbO_3$–$0.945Pb(Zr_{0.476}Ti_{0.524})O_3$ composition. However, the corresponding $T_c$ also drops rapidly from 590 °C for the

*Corresponding author. Tel./fax: +86 1062334195.
**Corresponding author. Tel./fax: +86 10 82547679.
*E-mail addresses:* bpzhang@ustb.edu.cn (B. Zhang), dong.guo@mail.ioa.ac.cn (D. Guo).

0272-8842/$ - see front matter © 2013 Elsevier Ltd and Techna Group S.r.l. All rights reserved.
http://dx.doi.org/10.1016/j.ceramint.2013.10.043

former ceramic to 390 °C for the latter one, indicating an incompatibly varying trend between each other. Developing high $T_c$ piezoelectric materials by synchronously enhancing $T_c$ and $d_{33}$ to find applications in various modern devices is still a great challenge.

$Fe_2O_3$ is usually doped in PZT-based ceramics as an acceptor [15], which could substitute B-site ions because of its comparable ionic size with those of $Ti^{4+}$ and $Zr^{4+}$ or as a sintering aid to improve sinterability [16]. The relative density of the $Pb_{0.95}Bi_{0.03}Nb_{0.02}Zr_{0.51}Ti_{0.49-x}Fe_xO_3$ ceramics was enhanced to over 97% by doping 6 at% $Fe_2O_3$ along with a high piezoelectric constant $d_{33}$ of 530 pm/V and electromechanical coupling factor $k_p$ of 0.638 [16]. An improved piezoelectric constant $d_{33}$ from 802 pC/N to 956 pC/N is achieved by doping 1.2 mol% $Fe_2O_3$ in the PNN–PZT system along with a high $k_p$ of 0.74 [17]. The highest $T_c$ of 451 °C and $d_{33}$ of 398 pC/N are attained in the Fe-doped BS–PT ceramics [18]. Fe was also used as a hard dopant for the BSPT based ternary high Tc ceramics [32]. It was reported that the complex effects of phase structure, grain size, and oxygen vacancy caused by the addition of $Fe_2O_3$ contribute to the improved piezoelectric property [15–18], which has been rarely studied in the BY–PZT piezoelectric ceramics so far. In the present study, the microstructure and electrical properties of $Fe_2O_3$-added $0.055BiYbO_3$–$0.945Pb(Zr_{0.476}Ti_{0.524})O_3$ (BY–PZT) piezoelectric ceramics were investigated with a special emphasis on the influence of $Fe_2O_3$ content.

## 2. Experimental

A series of $0.055BiYbO_3$–$0.945Pb(Zr_{0.476}Ti_{0.524})O_3+x$(mol%) $Fe_2O_3$ (abbreviated as BY–PZT–$x$Fe, $x$=0, 0.2, 0.4, 0.6, 0.8, 1.0 and 1.5) ceramics were prepared by conventionally mixed oxide ceramic processing techniques. Analytical pure $Bi_2O_3$, $Yb_2O_3$, $Pb_3O_4$, $TiO_2$, $ZrO_2$ and $Fe_2O_3$ were used as starting materials. The powders were weighed according to the nominal compositions, with 1 wt% excess amounts of $Bi_2O_3$ and $Pb_3O_4$ to compensate the volatilization during sintering. The mixtures were ball-milled for 18 h, dried and calcined at 750 °C for 3 h. Thereafter, calcined powders were remixed and pressed into disks 12 mm in diameter and 1.5 mm in thickness under 40 MPa using 2 wt% polyvinyl alcohol as binder, followed by burning the binder at 650 °C for 1 h and sintering at 1150 °C for 3 h. Phase structure was detected by using X-ray diffraction (XRD) with a Bruker D8 Advance instrument with Cu $K_{\alpha 1}$ radiation. The microstructure of the fresh fractured surfaces of sintered samples was examined by using scanning electron microscopy (SEM, Hitachi S-4800, Japan).

Both surfaces of the sintered discs were grounded, polished, then pasted with silver, and fired at 720 °C for 30 min. The sintered samples were poled at 140 °C for 20 min in a dc field of 4 kV/mm in silicone oil. The piezoelectric properties were measured after 24 h aging at room temperature. The piezoelectric constant $d_{33}$ was measured using a quasistatic piezoelectric $d_{33}$-meter (Model ZJ-3D, Institute of Acoustics, China). The temperature dependences of dielectric constant $\varepsilon_r$ and dielectric loss $\tan\delta$ were measured at 1 kHz using a HP4294A impedance analyzer from room temperature to 500 °C. The planar electromechanical coupling factor $k_p$ and the mechanical quality factor $Q_m$ were measured at room temperature by using the resonance and anti-resonance method techniques on the basis of IEEE standards. The ferroelectric polarization hysteresis loop was measured using an Radiant Precision LC ferroelectric testing system (Sawyer–Tower) in silicon oil at room temperature.

## 3. Results and discussion

Fig. 1 shows the XRD patterns of BY–PZT–$x$Fe ceramics. All samples consist of a perovskite main phase whose diffraction patterns are consistent with the standard card $PbZr_{0.4}Ti_{0.6}O_3$ (PDF#70-4264) with tetragonal symmetry especially for the sample of $x=0$. Apart from the tetragonal character of an obvious splitting of (002)/(200) peaks at $2\theta$ of about 45°, a shift trend of diffraction peaks is also noticed with increasing $x$ as

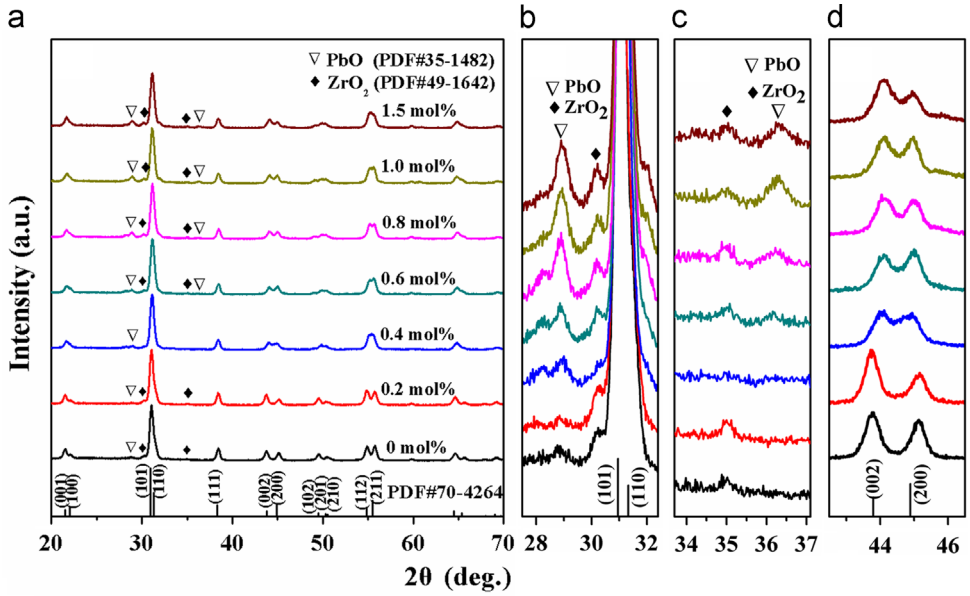


Fig. 1. X-ray diffraction patterns of the BY–PZT–$x$Fe ceramics.

highlighted in Fig. 1d, revealing a varied tetragonality (*c*/*a*) which will be discussed later. Some weak diffraction peaks deriving from the raw materials of PbO (∇, PDF#35-1482) and $ZrO_2$ (♦, PDF#49-1642) are also noticed in the samples as shown in Fig. 1b and c. The intensity of diffraction peaks for the PbO and $ZrO_2$ phases first decreased and then increased with increasing *x*, which indicates that the compositions of $x=0.4$ have the fewest impurity phase. Although no any corresponding Fe-containing impurity was detectable in all samples, it is easy to consider that there are two possibilities regarding the presence of $Fe^{3+}$ in BY–PZT–*x*Fe ceramics regardless of the low doping level of $Fe_2O_3$. One is to form a solid solution via diffusing $Fe^{3+}$ into lattices of the main phase, and the other may form a Fe-containing impurity which was undetected within the detection limit of the XRD.

Fig. 2 shows a further detailed change on the lattice parameters (*a* and *c*) as well as the tetragonality (*c*/*a*) for the BY–PZT–*x*Fe ceramics as a function of *x*. The parameters *a* and *c* of the main phase are the average values calculated from five peaks from $2\theta$ of 20° to 58° in the XRD patterns. As shown in Fig. 2a, a decreased *c* parameter is noticed at the compositions $0 \le x \le 0.4$ along with an increased *a*, corresponding to an obviously decreased *c*/*a* from 1.0296 to 1.0207 as shown in Fig. 2b. Since the ionic radius of $Fe^{3+}$ (0.645 Å) is smaller than those of $Ti^{4+}$ (0.68 Å) and $Zr^{4+}$ (0.79 Å), if $Fe^{3+}$ partially substitutes for $Zr^{4+}$ and $Ti^{4+}$, the perovskite lattice will shrink, which is also the contributing factor to the dramatically decreased *c*/*a*. Besides, the *c* parameter shows a moderate downward tendency beyond $x=0.4$ along with a steady *a* parameter, resulting in a slightly dropped *c*/*a* which lies in the range from 1.0181 to 1.016 for the samples of $x \ge 0.4$. Since the change in the $Zr^{4+}$ content or the ratio of $Zr^{4+}/Ti^{4+}$ in tetragonal host phase should produce more varied lattice parameters *a* and *b* rather than *c*, the nearly constant *a* and *b* values reveal that the real composition of tetragonal host phase should be constant regardless of the increased PbO and $ZrO_2$ impurities as $x \ge 0.4$ as shown in Fig. 2b. The effect of partial substitution of $Fe^{3+}$ for $Zr^{4+}$ and $Ti^{4+}$ should be absent owing to the solid solubility limitation of $Fe^{3+}$ at $x \ge 0.4$ in the perovskite phase. Hence, the $Fe_2O_3$ phase may remain at the same extent although it was undetected in the XRD pattern. The higher $Fe_2O_3$ content should reduce the sintering activity due to the high melting point of 1565 °C, whereby the residual PbO and $ZrO_2$ impurities show an increasing tendency to different degrees as shown in Fig. 1b and 1c. On the other hand, the nearly composition independent *a* and *b* values reveal that the real composition of tetragonal host phase should be constant regardless of the increased PbO and $ZrO_2$ impurities. Alternatively, the presence of another compensation behavior is also possible in order to keep nearly constant *a* and *b* values. The slightly increased $ZrO_2$ impurity should reduce the $Zr^{4+}$ content in host phase and lead to the decrease of *a* and *b* values, while the absence or insufficient replacement of smaller-sized $Fe^{3+}$ ions for $Zr^{4+}$ and $Ti^{4+}$ should alleviate the shrinkage of the perovskite lattice and compensate the decrease of *a* and *b* values. In a word, the *c*/*a* could be optimized by adding appropriate $Fe_2O_3$ content, which can modify BY–PZT ceramic's properties as discussed later.

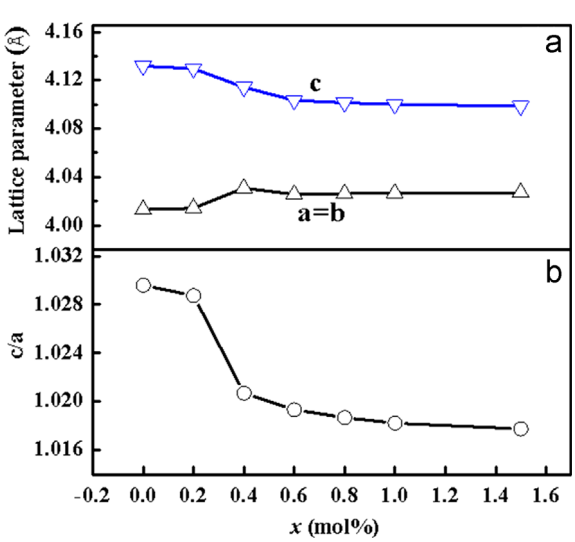


Fig. 2. Lattice parameters (a) and *c*/*a* (b) of the BY–PZT–*x*Fe ceramics.

Fig. 3 shows typical SEM pictures of the fresh fractured surfaces for the BY–PZT–*x*Fe ceramics. A better crystallinity with complete grain growth and dense microstructure appears in all samples. The sample with $x=0$ shown in Fig. 3a possesses inhomogeneous grains. The small grains grow up gradually and the grain size tends to be uniform with increasing *x* from 0 to 0.4 because of the enhanced sintering activity via the partial substitution of $Fe^{3+}$ for $Zr^{4+}$ and $Ti^{4+}$. While the grain sizes inversely decrease with further increasing *x* to 1.5, which may be ascribed to the increased impurity phase (Fig. 1b and c) since the $Fe^{3+}$ may reach the solid solubility limitation in the perovskite structure for $x \ge 0.4$. The impurity phase will impede grain growth and lead to a decreased density with refined grains. The relative density of the BY–PZT–*x*Fe samples (when $x=0$, 0.2, 0.4, 0.6, 0.8, 1.0 and 1.5) was 94.23%, 94.66%, 95.49%, 90.38%, 89.99%, 89.57% and 89.55%, respectively. It is obvious that excessive $Fe_2O_3$ ($x > 0.4$) not only decreases the relative density but also suppresses the grain growth (Fig. 3d and f).

Fig. 4 shows the electrical properties of BY–PZT–*x*Fe ceramics. The piezoelectric constant $d_{33}$ and planar electromechanical coupling factor $k_p$ show an initially increased tendency and then a decreased one with increasing *x*. Both $d_{33}$ and $k_p$ reach the maximum values of 175 pC/N and 0.3027 at $x=0.4$, respectively. And the $d_{33}$ of 175 pC/N is significantly greater than that (18 pC/N) of isostructural $0.1BiYbO_3$–$0.9PbTiO_3$ piezoelectric ceramics [9]. The mechanical quality factor $Q_m$ shows an inversely varying tendency to the $d_{33}$ and $k_p$ with increasing *x*, and the minimum value of 92.5 and the maximum one of 128.8 are attained at $x=0.4$ and 1.5, respectively. As shown in Fig. 2, the lattice parameter *a* increases and *c* decreases along with the decreased *c*/*a* by increasing *x* from 0 to 0.4, while the lattice parameters *a*, *c* and *c*/*a* ratio are steady beyond $x=0.4$. Generally, the large tetragonal distortion will seldomly benefit the piezoelectric activity for the PZT ceramics system. However, the decreased *c*/*a* can improve poling conditions due to the decreased coercive field [19]. Hence, the decreased *c*/*a* will make the phase structure of the ceramics closer to that of the MPB composition, which will be beneficial to the polarization of the ferroelectric or reactive ions ($Ti^{4+}$ or $O^{2-}$); thereby it is more conducive to enhancing the large piezoelectric activity of the ceramic system. Meanwhile, the grain sizes in Fig. 3c and the

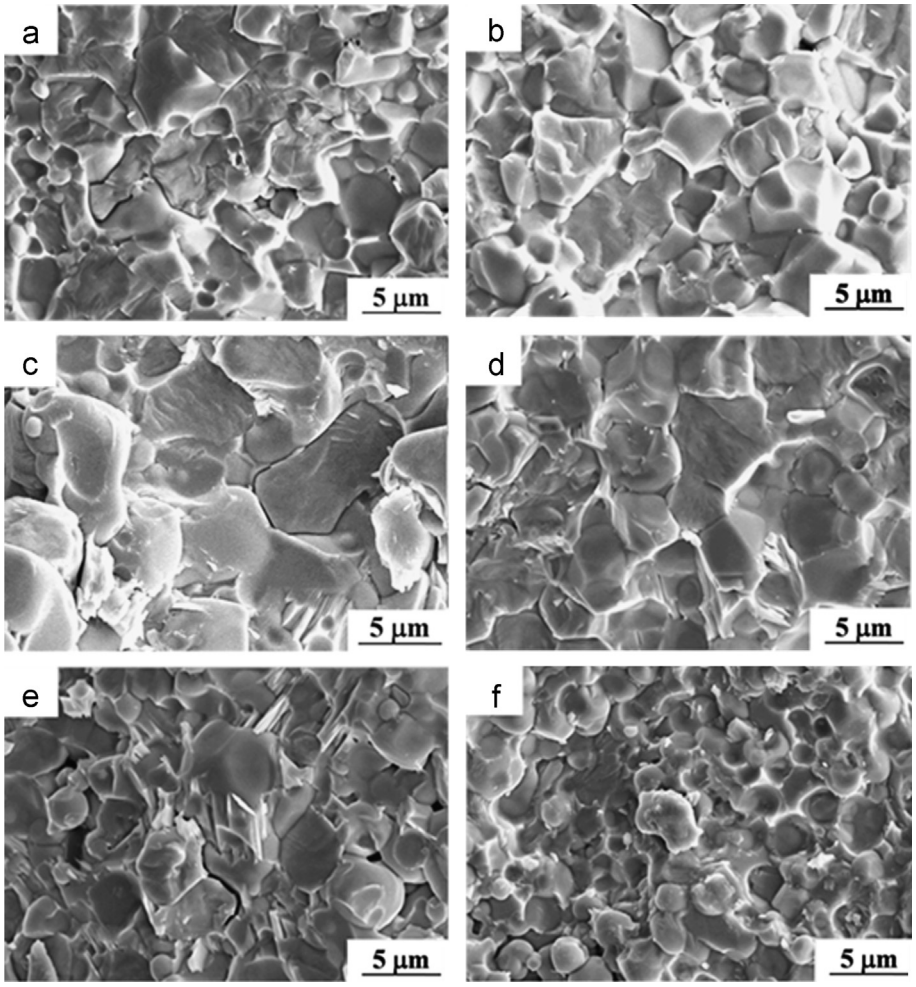


Fig. 3. SEM images of the fracture surfaces for the BY–PZT–$x$Fe ceramics: (a) $x=0$, (b) $x=0.2$, (c) $x=0.4$, (d) $x=0.6$, (e) $x=0.8$ and (f) $x=1.5$.

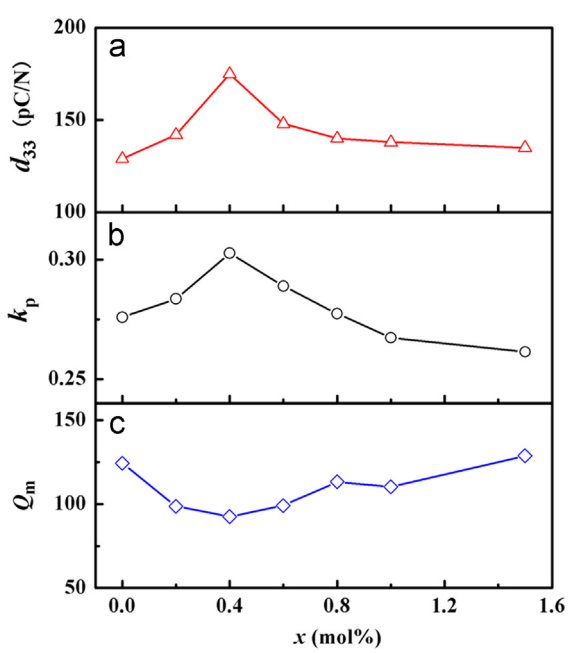


Fig. 4. Piezoelectric constant $d_{33}$ (a), planar electromechanical coupling factor $k_p$ (b), and mechanical quality factor $Q_m$ (c) of the BY–PZT–$x$Fe ceramics.

relative density reach the maximum values at $x=0.4$, which is also in favor of enhancing the piezoelectric response. On the other hand, as shown in Fig. 1b and c, a tiny amount of impurity phase also restricts the effect on inhibiting piezoelectric properties. Moreover, the movement of the domain is also relatively easy with larger mechanical energy loss in the phase boundary, resulting in the minimum $Q_m$ at $x=0.4$. However, the amount of impurity phase increases obviously for the $x \geq 0.4$ components with refined grains and decreased density, which will weaken the piezoelectric properties along with the decreased $d_{33}$ and $k_p$. Further increasing $x$ leads to a gradually increased $Q_m$ , showing a "hard" characteristic. This may be due to the low valence substitution of $Fe^{3+}$ for $Zr^{4+}$ and $Ti^{4+}$, which will lead to the appearance of oxygen vacancies in order to maintain electro-valence balance. The oxygen vacancies will produce a "pinning effect" on the domain rotation, thereby the material becomes "hard". Moreover, the electrical properties of the BY–PZT–$x$Fe ceramics are related to the grain size, density as well as the phase structure, including the perovskite symmetry and the impurity phase which are related to the doped $Fe_2O_3$. The improvement of piezoelectric response ($d_{33}$ and $k_p$) at $x=0.4$ is attributed to the more stable perovskite symmetry with a low $c/a$, better grain

morphology, and higher density as well as the rare impurity phases.

Fig. 5 shows the relationship between the $d_{33}$ and $T_c$ for the reported high $T_c$ piezoceramics. The bismuth layer-structured compounds $Bi_{7-x}Nd_xTi_4NbO_{21}$ possess an extremely high $T_c$ above 750 °C while a lower $d_{33}$ of 16.3 pC/N at $x=1.25$ [20]. The perovskite structured solid solution, such as BIPT, has a high $T_c$ of 542 °C and $d_{33}$ of 60 pC/N [21]. A high $T_c$ of about 525 °C was also noticed in the tungsten bronze structure $Pb_{0.94}La_{0.06}Nb_2O_6$ ceramics with $d_{33}=62.3$ pC/N, $k_p=0.3342$ and $Q_m=11.64$ [22]. Among these high $T_c$ piezoelectric ceramics, the $BiYbO_3$–$PbTiO_3$ (BY–PT) is an attractive candidate due to its high $T_c$ up to 590 °C and lower cost [9]. Lots of modified BY–PT piezoelectric ceramics around $0.1BiYbO_3$–$0.9PbTiO_3$ composition have shown a great potential for high temperature piezoelectric applications [23]. In this study, the BY–PZT–$x$Fe ceramics at $x=0$, 0.2 and 0.4 show a higher $d_{33}$ up to 129–175 pC/N than those for $0.1BiYbO_3$–$0.9PbTiO_3$ ($d_{33}=18$ pC/N) [9] and $0.88(0.1BiYbO_3$–$0.9PbTiO_3)$–$0.12BaTiO_3$ ($d_{33}=34$ pC/N) [23], along with a $T_c$ up to 350–390 °C superior to those of PZT-based ceramics [24–28]. Due to a lower tetragonality $c/a$, better grain morphology, and higher density as well as the limited impurity phase, the $x$=0.4 composition showed a high Curie temperature $T_c$ up to 350 °C and good piezoelectric properties with $d_{33}$ reaching 175 pC/N, indicating promising applications in the high-temperature piezoelectric devices.

Fig. 6 shows the polarization–electric field ($P$–$E$) hysteresis loops of BY–PZT–$x$Fe ceramics at room temperature. An unclosed and significantly asymmetric $P$–$E$ loop appears at $x=0.6$, showing a quite weakened ferroelectricity, which is also similar to its other counterparts at $0.8 \le x \le 1.5$ with an intensive asymmetry. This indicates that there is polarization charge in the ceramic itself to increase leakage current, which is due to the increased impurity phase content, and refined grains as well as decreased density. It is worth noting that the $P$–$E$ loop shows a saturation tendency at $x=0$ and 0.4; the remnant polarization $P_r$ and the coercive field $E_c$ increase with increasing $x$. The maximum $P_r$ is 12 μC/cm$^2$ at $x=0.4$ with an $E_c$ =26.8 kV/cm. The high $E_c$ shows a "hard" feature, which is attributed to the acceptor doping of $Fe^{3+}$ in BY–PZT–$x$Fe ceramics because of

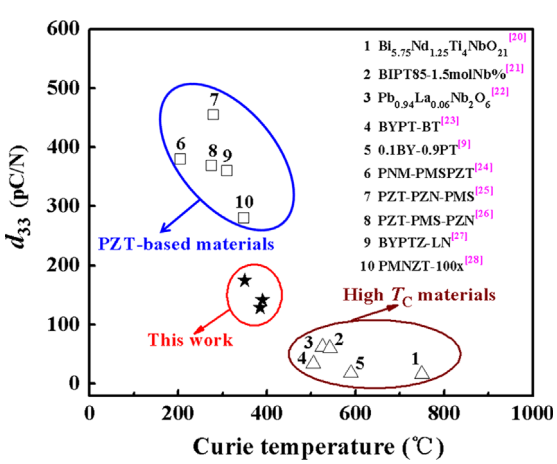


Fig. 5. Relationship between the piezoelectric constant $d_{33}$ and Curie temperature $T_c$ for the reported high $T_c$ piezoceramics.

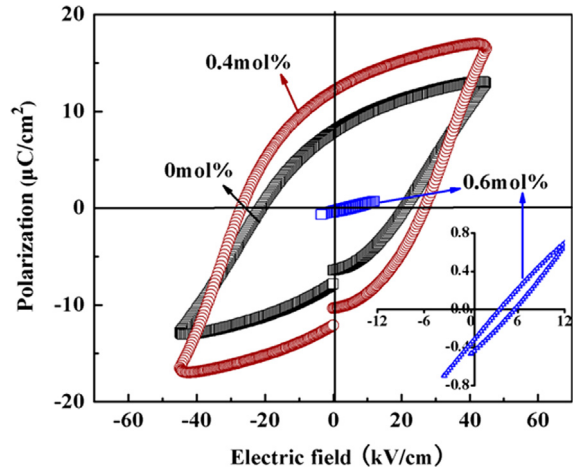


Fig. 6. Polarization–electric field ($P$–$E$) hysteresis loops of the BY–PZT–$x$Fe ceramics at room temperature.

the low valence substitution of $Fe^{3+}$ for $Zr^{4+}$ and $Ti^{4+}$ in the B-site of the perovskite lattice. Moreover, since the ionic radius of $Fe^{3+}$ (0.645 Å) is smaller than those of $Ti^{4+}$ (0.68 Å) and $Zr^{4+}$ (0.79 Å), the substitution of a small amount of $Fe^{3+}$ for $Zr^{4+}$ and $Ti^{4+}$ should result in the formation of partial metastable B–O bonds, making the ferroelectric domain flip easier, increasing $P_r$. The high density and optimal solid solution effect of $Fe^{3+}$ are also conducive for a good ferroelectric at the $x=0.4$ composition.

Fig. 7 shows the temperature dependence of dielectric constant $\varepsilon_r$ and dielectric loss $\tan\delta$ for the BY–PZT–$x$Fe ceramics at 1 kHz. The $\varepsilon_r$ in Fig. 7a for BY–PZT–$x$Fe samples at $0 \le x \le 0.4$ increases slowly from room temperature to 300 °C, and then rapidly increases over 300 °C, exhibiting a relatively sharp dielectric peak. This transition corresponds to the ferroelectric–paraelectric phase transformation at $T_c$ which is 385 °C, 390 °C and 350 °C for samples of $x=0$, 0.2 and 0.4, respectively. With increasing $x$, the $T_c$ first increased slightly from 385 °C to 390 °C and then declined significantly to 350 °C, which almost corresponds to the tendency of $c/a$ ratio in Fig. 2b. It is well known that $T_c$ depends on the $c/a$ ratio and decreases with the diminution of the tetragonality [29–31]. Generally, the increased tetragonal distortion is attributed to the increased position deviation of the A-site ion center in the $ABO_3$ perovskite structure, causing the increased internal energy of systems. Therefore, it requires a higher energy, i.e. a higher temperature, for the ferroelectric–paraelectric phase transition, which is also the reason for increasing $T_c$ [19]. Apart from the decreased $T_c$ for samples at $x>0.4$, the dielectric peaks are significantly wider with a decreased permittivity maximum value, which may be attributed to the increased impurities such as PbO, $ZrO_2$ and $Fe_2O_3$. A double dielectric peak appears for $x=0.6$ mol%, whose $P$–$E$ loop also indicates an unclosed and significantly asymmetric profile as shown in the inset of Fig. 6, indicating that a double dielectric peak may correspond to a quite weakened ferroelectricity in BY–PZT–$x$Fe ceramics. Both of them may relate to refined grains and decreased density besides the increased impurities. In addition, the appearance of a double dielectric peak suggests a diffuse phase transition characteristic from normal ferroelectric to relaxor

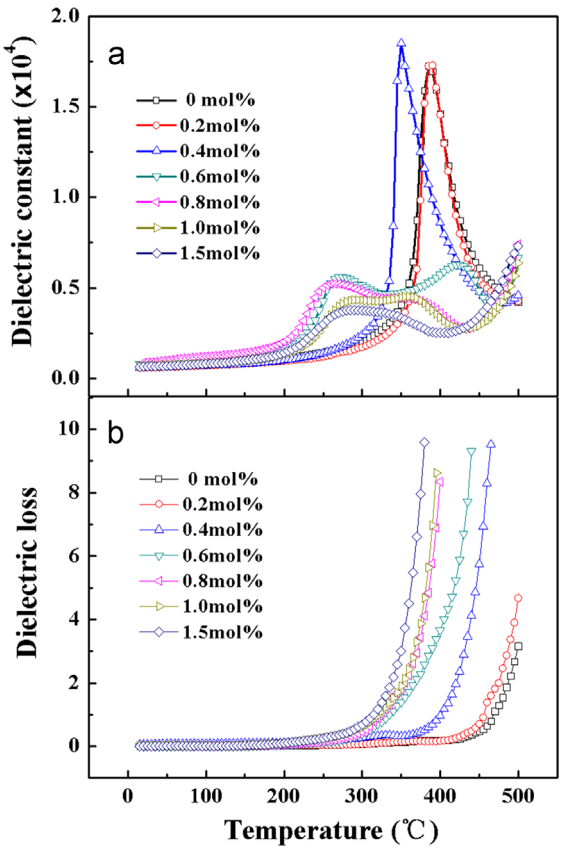


Fig. 7. Temperature dependence of dielectric constant ($\varepsilon_r$) (a) and dielectric loss (tan $\delta$) (b) at 1 kHz for the BY–PZT–$x$Fe ceramics.

ferroelectric which may be caused by different impurities with high content and is still unknown. The tan $\delta$ in Fig. 7b shows a similar low value of 0.007 over the wide temperature range of room temperature to 300 °C for all samples, exhibiting good temperature stability. A sharply increased tan $\delta$ value is noticed near $T_c$, indicating an obvious increase in dc conductivity at high temperatures. The $T_c$ up to 350–390 °C superior to that of PZT as well as a higher $d_{33}$ up to 129–175 pC/N than that of the reported BY–PT counterparts [9]suggests this to be a candidate for increased temperature piezoelectric applications, although containing some unexpected impurity compared with recently reported high-$T_c$ piezoelectric ceramic systems. Therefore, it is expectable that the electrical properties should be further enhanced by forming a single perovskite structure via optimized preparing process and so on.

## 4. Conclusion

A series of $0.055BiYbO_3$–$0.945Pb(Zr_{0.476}Ti_{0.524})O_3+x$(mol%) $Fe_2O_3$ (BY–PZT–$x$Fe) piezoelectric ceramics were prepared by conventionally mixed oxide ceramic processing techniques. The phase structure and electrical properties were investigated with a special emphasis on the influence of $Fe_2O_3$ content. All samples had a perovskite main phase with tetragonal symmetry along with a tiny amount of PbO and $ZrO_2$ impurities. The partial substitution of $Fe^{3+}$ for $Zr^{4+}$ and $Ti^{4+}$ in the B-site caused the shrinkage of perovskite lattice and a decreased tetragonality ($c/a$) with increasing $x$ up to the solid solubility saturation at $x=0.4$. A lower tetragonality ($c/a$), better grain morphology, and higher density as well as the limited impurity phases were achieved at $x=0.4$ composition, which all contribute to the most improved piezoelectric properties. The BY–PZT–$x$Fe ceramics at $x=0$–0.4 showed a higher $d_{33}$ up to 129–175 pC/N than that of the reported BYPT counterparts, along with a $T_c$ up to 350–390 °C superior to that of PZT. The result suggests that the BY–PZT–$x$Fe ceramics are an alternative for high temperature piezoelectric applications compared with other recently reported high-$T_c$ piezoelectric ceramics.

## Acknowledgments

This work was supported by the "100 Talented Program" of Chinese Academy of Sciences, the National Key Basic Research Program of China (973 Program, Grant no. 2013CB632900) and the National Science Foundation of China (NSFC No. 11074277). The authors also thank the open foundation of the state key laboratory of new ceramics and fine processing of Tsinghua University.

## References

[1] R.C. Turner, P.A. Fuierer, R.E. Newnham, T.R. Shrout, Materials for high temperature acoustic and vibration sensors: a review, J. Appl. Acoust. 41 (1994) 299.
[2] T. Leist, J. Chen, W. Jo, E. Aulbach, J. Suffner, J. Rodel, Temperature dependence of the piezoelectric coefficient in $BiMeO_3$–$PbTiO_3$ (Me=Fe, Sc, $(Mg_{1/2}Ti_{1/2})$) ceramics, J. Am. Ceram. Soc. 95 (2) (2012) 711–715.
[3] A.Z. Simoes, A.H.M. Gonzalez, A.A. Cavalheiro, Effect of magnesium on structure and properties of $LiNbO_3$ prepared from polymeric precursors, Ceram. Int. 28 (2002) 265–270.
[4] R.E. Eitel, C.A. Randall, T.R. Shrout, P.W. Rehrig, et al., New high temperature morphotropic phase boundary piezoelectrics based on Bi(Me)$O_3$–$PbTiO_3$ ceramics, Jpn. J. Appl. Phys. 40 (2001) 5999–6002.
[5] S. Chen, X. Dong, H. Yang, R. Liang, C. Mao, Effects of niobium doping on the microstructure and electrical properties of $0.36BiScO_3$–$0.64PbTiO_3$ ceramics, J. Am. Ceram. Soc. 90 (2) (2007) 477–482.
[6] C.A. Randall, R.E. Eitel, T.R. Shrout, D.I. Woodward, I.M. Reaney, Transmission electron microscopy investigation of the high temperature $BiScO_3$–$PbTiO_3$ piezoelectric ceramic system, J. Appl. Phys. 93 (2003) 9271–9274.
[7] R.E. Eitel, S.J. Zhang, T.R. Shrout, C.A. Randall, I. Levin, Phase diagram of the perovskite system $(1-x)BiScO_3$–$xPbTiO_3$, J. Appl. Phys. 96 (2004) 2828–2831.
[8] R.E. Eitel, C.A. Randall, T.R. Shrout, S.E. Park, Preparation and characterization of high temperature perovskite ferroelectrics in the solid–solution $(1-x)BiScO_3$–$xPbTiO_3$, Jpn. J. Appl. Phys. 41 (2002) 2099–2104.
[9] F. Gao, R.Z. Hong, J.J. Liu, Z. Li, L.H. Cheng, C.H. Tian, Phase formation and characterization of high Curie temperature $xBiYbO_3$–$(1-x)PbTiO_3$ piezoelectric ceramics, J. Eur. Ceram. Soc. 29 (2009) 1687–1693.
[10] R. Duan, R.F. Speyer, E. Alberta, T.R. Shrout, High Curie temperature perovskite $BiInO_3$–$xPbTiO_3$ ceramics, J. Mater. Res. 19 (7) (2004) 2185–2192.
[11] J.R. Cheng, W. Zhu, N. Li, L.E. Cross, Fabrication and characterization of $xBiGaO_3$–$(1-x)PbTiO_3$: a high temperature reduced Pb-content piezoelectric ceramic, Mater. Lett. 57 (2003) 2090–2094.
[12] J.R. Cheng, N. Li, L.E. Cross, Structural and dielectric properties of Ga-modified $BiFeO_3$–$PbTiO_3$ crystalline solution, J. Appl. Phys. 94 (8) (2003) 5153–5157.

[13] P. Comyn, S.P. McBride, A.J. Bell, Processing and electrical properties of $BiFeO_3$–$PbTiO_3$ ceramics, Mater. Lett. 58 (2004) 3844–3846.
[14] L. Yang, F. Gao, Z.Q. Deng, C.S. Tian, Effect of $PbZrO_3$ on the phase structure and electrical properties of $0.1BiYbO_3$–$0.9PbTiO_3$ piezoelectric ceramics, Piezo Acous. 32 (2010) 647–653.
[15] S.J. Yoon, A. Joshi, K. Uchino, Effect of additives on the electromechanical properties of $Pb(Zr,Ti)O_3$–$Pb(Y_{2/3}W_{1/3})O_3$ ceramics, J. Am. Ceram. Soc. 80 (1997) 1035–1039.
[16] C. Miclea, C. Tanasoiu, C.F. Miclea, L. Amarande, A. Gheorghiu, F.N. Sima, Effect of iron and nickel substitution on the piezoelectric properties of PZT type ceramics, J. Eur. Ceram. Soc. 25 (2005) 2397–2400.
[17] J.Z. Du, J.H. Qiu, K.J. Zhu, H.L. Ji, X.M. Pang, J. Luo, Effects of $Fe_2O_3$ doping on the microstructure and piezoelectric properties of $0.55Pb(Ni_{1/3}Nb_{2/3})O_3$–$0.45Pb(Zr_{0.3}Ti_{0.7})O_3$ ceramics, Mater. Lett. 66 (2012) 153–155.
[18] P. Winotai, N. Udomkan, S. Meejoo, Piezoelectric properties of $Fe_2O_3$-doped $(1-x)BiScO_3$–$xPbTiO_3$ ceramics, Sensor Actuat. A: Phys. 122 (2005) 257–263.
[19] Z.H. Yao, L.Y. Peng, H.X. Liu, H. Hao, M.H. Cao, Z.Y. Yu, Relationship between structure and properties in high-temperature $Bi(Al_{0.5}Fe_{0.5})O_3$–$PbTiO_3$ piezoelectric ceramics, J. Alloys Compd. 509 (2011) 5637–5640.
[20] C.W. Shao, Y.Q. Lu, D. Wang, Y.X. Li, Effect of Nd substitution on the microstructure and electrical properties of $Bi_7Ti_4NbO_{21}$ piezoceramics, J. Eur. Ceram. Soc. 32 (2012) 3781–3789.
[21] S.J. Zhang, R. Xia, C.A. Randall, T.R. Shrout, Dielectric and piezoelectric properties of niobium-modified $BiInO_3$–$PbTiO_3$ perovskite ceramics with high Curie temperatures, J. Mater. Res. 20 (2005) 2067–2071.
[22] X.M. Chen, X.G. Zhao, W. Ding, P. Liu, Microstructure and dielectric properties of $Pb_{0.94}La_{0.06}Nb_2O_6$ ceramics, Ceram. Int. 37 (2011) 2855–2859.
[23] F. Gao, R.Z. Hong, J.J. Liu, Z. Li, L.H. Cheng, C.H. Tian, Phase structure and piezoelectric properties of high Curie temperature $BiYbO_3$–$PbTiO_3$–$BaTiO_3$ ceramics, J. Alloys Compd. 475 (2009) 619–623.
[24] H.L. Du, Z.B. Pei, W.C. Zhou, F. Luo, S.B. Qu, Effect of addition of $MnO_2$ on piezoelectric properties of PNW–PMS–PZT ceramics, Mater. Sci. Eng. A 421 (2006) 286–289.
[25] Z.P. Yang, Y.F. Chang, H. Li, Piezoelectric and dielectric properties of PZT–PZN–PMS ceramics prepared by molten salt synthesis method, Mater. Res. Bull. 40 (2005) 2110–2119.
[26] Z.P. Yang, H. Li, X.M. Zong, Y.F. Chang, Structure and electrical properties of PZT–PMS–PZN piezoelectric ceramics, J. Eur. Ceram. Soc. 26 (2006) 3197–3202.
[27] F. Gao, Z.Q. Deng, L. Yang, L.H. Cheng, C.S. Tian, Phase transitional behavior and piezoelectric properties of $BiYbO_3$–$Pb(Ti_{0.5}Zr_{0.5})O_3$–$LiNbO_3$ ceramics, Ceram. Int. 35 (2009) 2885–2890.
[28] C.C. Tsai, S.Y. Chu, C.K. Liang, Low-temperature sintered PMnN–PZT based ceramics using the B-site oxide precursor method for therapeutic transducers, J. Alloys Compd. 478 (2009) 516–522.
[29] C.J. Stringer, T.R. Shrout, C.A. Randall, I.M. Reaney, Classification of transition temperature behavior in ferroelectric $PbTiO_3$–$Bi(Me'Me'')O_3$ solid solutions, J. Appl. Phys. 99 (2006) 024106 (4).
[30] H. Wang, B. Wang, Q.K. Li, et al., First-principles study of the cubic perovskites $BiMO_3$ (M = Al, Ga, In, and Sc), Phys. Rev. B 75 (2007) 245209 (245209).
[31] S.J. Zhang, F.P. Yu, Piezoelectric materials for high temperature sensors, J. Am. Ceram. Soc. 94 (2011) 3153–3170.
[32] Q.W. Liao, X.S. Chen, X.C. Chu, F. Zeng, Dong Guo, Effect of Fe doping on the structure and electric properties of relaxor type BSPT-PZN piezoelectric ceramics near the morphotropic phase boundary, Sensor. Actuat. A Phys. 201 (2013) 222–229.